Chandra Multiwavelength Project (ChaMP)
X-ray Point Source Number Counts and the Cosmic X-ray Background

Minsun Kim[1,2], Belinda J. Wilkes[2], Dong-Woo Kim[2], Paul J. Green[2], Wayne A. Barkhouse[3], Myung-Gyoon Lee[1], John D. Silverman[4], and Harvey D. Tananbaum[2]
[1]Seoul National University, [2]Harvard-Smithsonian Center for Astrophysics,
[3]University of Illinois at Urbana-Champaign, [4]Max-Plank Institute for extraterrestrial Physics
mskim@astro.snu.ac.kr or mkim@cfa.harvard.edu

http://hea-www.harvard.edu/CHAMP

http://hea-www.harvard.edu/CHAMP

Abstract

We present the Chandra Multiwavelength Project (ChaMP) X-ray point source number counts and the cosmic X-ray background (CXRB) flux densities in multiple energy bands. From the ChaMP X-ray point source catalog, ~5,500 sources are selected covering 9.6 deg^2 in sky area. To quantitatively characterize the sensitivity and completeness of the ChaMP sample, we perform extensive simulations. We also include the ChaMP+CDFs (Chandra Deep Fields) number counts to cover large flux ranges from 2×10^{-17} to 2.4×10^{-12} (0.5-2 keV) and from 2×10^{-16} to 7.1×10^{-12} (2-8 keV) $erg\ cm^{-2}\ sec^{-1}$. The ChaMP and the ChaMP+CDFs differential number counts are well fitted with a broken power law. The best fit faint and bright power indices are $1.49^{+0.02}_{-0.02}$ and $2.36^{+0.05}_{-0.05}$ (0.5-2 keV), and $1.58^{+0.01}_{-0.01}$ and $2.59^{+0.06}_{-0.05}$ (2-8 keV), respectively. We detect breaks of the differential number counts and they appear at different fluxes in different energy bands. Assuming a single power law model for a source spectrum, we find that the same population(s) of soft X-ray sources causes the break in the differential number counts for all energy bands. We measure the resolved CXRB flux densities from the ChaMP and the ChaMP+CDFs number counts with and without bright target sources. Adding the known unresolved CXRB to the ChaMP+CDFs resolved CXRB, we also estimate total CXRB flux densities. The fractions of the resolved CXRB without target sources are 78 ± 1% and 81 ± 2% in the 0.5-2 keV and 2-8 keV bands, respectively. These fractions increase by ~1% when target sources are included.

I. ChaMP Data

The ChaMP X-ray point source catalog includes ~6,800 X-ray sources of 149 Chandra fields (Kim et al. 2006, ApJS submitted). To construct the ChaMP X-ray point source number counts, the sources in the I0, I1, I2, and I3 CCD chips for ACIS-I, and in the I2, I3, S2, and S3 CCD chips for ACIS-S of the main ChaMP X-ray point source catalog were selected. In addition, we selected the sources with a signal to noise ratio of S/N>1.5 corresponding to source counts>5. Our selection results in ~5,500 sources in the 0.3-8 keV band.

II. ChaMP/ChaMP+CDFs Number Counts

We derived the ChaMP cumulative/differential number counts in the 6 energy bands. To cover the wide flux range, we also derived the ChaMP+CDFs (see Bauer et al. 2004, AJ, 128, 2048 for CDFs) cumulative/differential number counts in 2 energy bands. The differential number counts are fitted well with a broken power law and the breaks are detected in every energy bands. Following figures show the ChaMP+CDFs number counts. The fitting results are plotted as red lines. Black and blue symbols represent CDFs and ChaMP number counts, respectively.

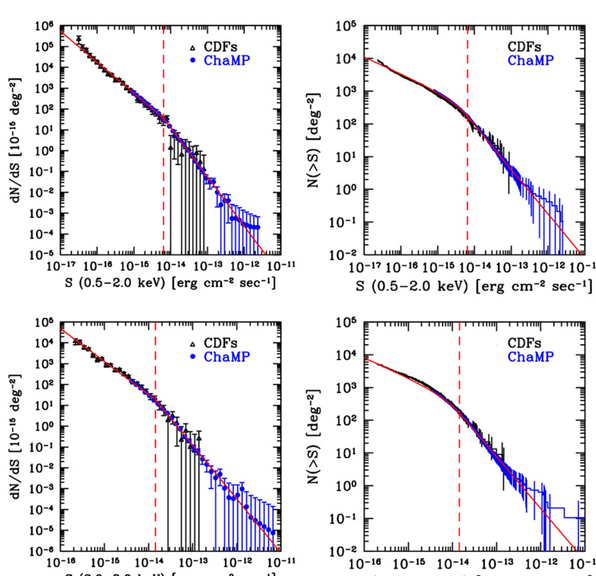

$$\frac{dN}{dS}=\begin{cases}K(S/S_{ref})^{-\gamma_1}, & S<S_b,\\ K(S_b/S_{ref})^{(\gamma_2-\gamma_1)}(S/S_{ref})^{-\gamma_2}, & S\geq S_b,\end{cases}$$

where, K is the normalization constant at flux $S_{ref}=10^{-15}$ $erg\ cm^{-2}\ sec^{-1}$, S_b is the break flux, and γ_1 and γ_2 are power index.

The ChaMP+CDFs number counts cover very wide flux ranges, $f_{0.5-2.0}=3\times10^{-17}\sim10^{-12}$ and $f_{2.0-8.0}=2\times10^{-16}\sim10^{-11}$ $erg\ cm^{-2}\ sec^{-1}$ with smaller statistical errors.

In the ChaMP and the ChaMP+CDFs differential number counts, the breaks are detected in all energy bands, and they appear at different flux levels in different energy bands.

III. Origin of Different Break Fluxes in Different Energy Bands

What is the origin of different break fluxes in different energy bands? The simplest explanation is that the break flux shifts as a function of energy band due to the corresponding flux levels in each band. To investigate this possibility, we estimate the expected break flux shift by rescaling the break flux in a given energy band into the other energy bands using an assumed X-ray source spectrum.

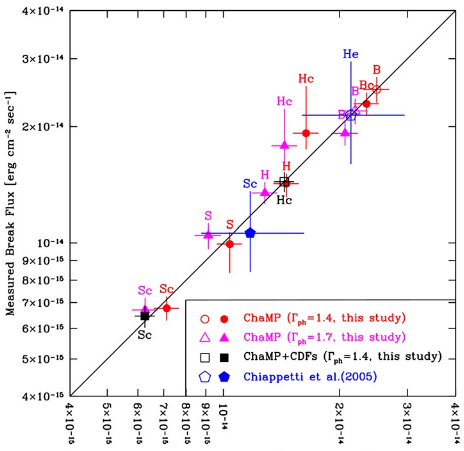

$$S_{b,exp}(E_1-E_2)=S_{b,std}\frac{\int_{E_1}^{E_2}E^{-\Gamma_{ph}}EdE}{\int_{E_{S1}}^{E_{S2}}E^{-\Gamma_{ph}}EdE}$$

where $S_{b,std}$ is a break flux in a standard E_{S1}-E_{S2} keV energy band and Γ_{ph} is the photon index of a spectrum. To calculate the expected break fluxes of the ChaMP and the ChaMP+CDFs, we used $S_{b,std}=2.5\times10^{-14}$ and $S_{b,std}=2.2\times10^{-14}$ $erg\ cm^{-2}\ sec^{-1}$ which are the measured break flux in the 0.3-8 keV band with photon indices of $\Gamma_{ph}=1.4$ and 1.7.

The measured and expected break fluxes agree within the uncertainties. Therefore, the break flux shifts as a function of energy band to the corresponding fluxes in each energy band and there is no need to invoke a different population to explain the shift.

VI. Cause of the Break

Harrison et al. (2003, ApJ, 596, 944) constructed the differential number counts in the 2-10 keV and found that the soft sources (HR<0) show a break while the hard (HR>0) sources do not. They suggested that, on average, the hard sources may be at lower redshift, and so do not show the cosmological evolutionary effects which cause the break. We investigated the HR dependence of the break flux for the ChaMP number counts in 6 energy bands.

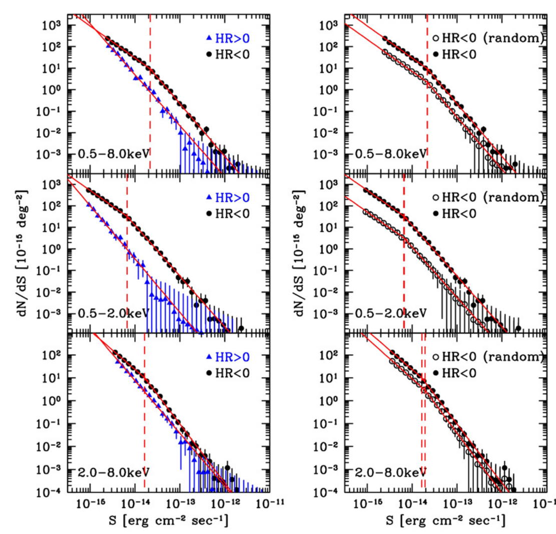

Left. Differential number counts for the soft (HR<0, black circles) and hard (HR>0, blue triangles) sources in 3 energy bands. **Soft sources show a break and are fitted with a broken power law while hard sources do not show a break and are fitted with a single power law.** Red solid lines are the best fit results. Red vertical dashed line is the break flux in the soft source number counts.
Right. Averaged differential number counts from 1,000 random subsets of soft sources (open circles). Each subset has the same number of soft sources as hard sources. Even with the reduced statistics, soft sources still show a significant break and are fitted with a broken power law. The number counts for all soft sources (filled circles) is plotted in each energy band for comparison.

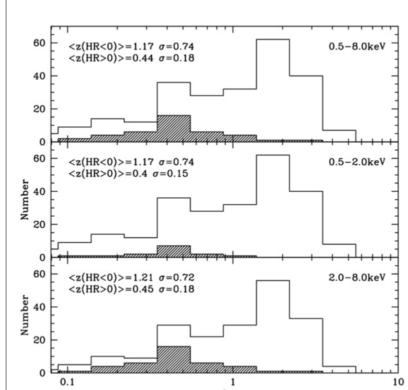

The redshift distributions of the soft (open histogram) and hard (shaded histogram) sources in 3 energy bands. **Hard sources are distributed at lower redshifts compared to the soft sources.** For these plots, ~300 ChaMP sources with the highest optical counterpart match confidence levels and with the highest spectrum quality are only used.

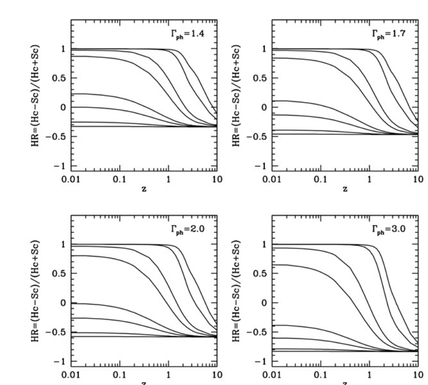

The hardness ratio of the test X-ray source as a function of redshift for photon indices of 1.4, 1.7, 3.0 and 4.0, respectively. In each panel, eight lines represent intrinsic absorptions of $\log N_{H,int}$=20, 21, 21.7, 22, 22.7, 23, 23.7, and 24, respectively, from bottom to top. **The source becomes harder with increasing intrinsic absorption and with increasing redshift. The intrinsically hard source with high redshift is observed as a soft source in the observed frame due to the cosmological redshift.**

V. Cosmic X-ray Background (CXRB)

Total CXRB flux density = Resolved CXRB flux density + Unresolved CXRB flux density

Table 9. The Total Cosmic X-ray Background Flux Density

Band (1)	Unresolved CXRB (2)	Unresolved CXRB [%] (3)	Resolved CXRB (4)	Resolved CXRB [%] (5)	Total CXRB (6)	Reference (7)
0.5-2	—	—	—	$94.3^{+7.0}_{-6.7}$	$0.75^{+0.04}_{-0.04}$	Moretti et al. 2003
2-10	—	—	—	$88.8^{+7.8}_{-6.6}$	$2.02^{+0.11}_{-0.11}$	
0.5-2	—	—	—	$89.5^{+5.9}_{-5.7}$	$0.75^{+0.04}_{-0.04}$	Bauer et al. 2004
2-8	—	—	—	$92.6^{+6.6}_{-6.3}$	$1.79^{+0.11}_{-0.11}$	
1-2	$0.10^{+0.01}_{-0.01}$	$22.7^{+3.1}_{-3.1}$	$0.35^{+0.02}_{-0.02}$	$77.0^{+3.0}_{-3.0}$	$0.46^{+0.03}_{-0.03}$	Hickox & Markevitch 2006
2-8	$0.34^{+0.17}_{-0.17}$	$20.0^{+10.0}_{-10.0}$	$1.36^{+0.10}_{-0.10}$	$80.0^{+8.0}_{-8.0}$	$1.70^{+0.20}_{-0.20}$	
0.5-2	$0.18^{+0.03}_{-0.03}$	$21.9^{+3.8}_{-3.8}$	$0.63^{+0.01}_{-0.01}$	$78.1^{+1.2}_{-1.2}$	$0.81^{+0.03}_{-0.03}$	this study
1-2	$0.10^{+0.01}_{-0.01}$	$21.5^{+2.9}_{-2.9}$	$0.38^{+0.01}_{-0.01}$	$78.5^{+1.2}_{-1.2}$	$0.48^{+0.02}_{-0.02}$	without targets
2-8	$0.34^{+0.17}_{-0.17}$	$19.5^{+9.8}_{-9.8}$	$1.40^{+0.03}_{-0.03}$	$80.5^{+1.7}_{-1.7}$	$1.74^{+0.17}_{-0.17}$	
0.5-2	$0.18^{+0.03}_{-0.03}$	$20.7^{+3.6}_{-3.6}$	$0.68^{+0.01}_{-0.01}$	$79.3^{+1.2}_{-1.2}$	$0.86^{+0.03}_{-0.03}$	this study
1-2	$0.10^{+0.01}_{-0.01}$	$20.2^{+2.7}_{-2.7}$	$0.41^{+0.01}_{-0.01}$	$79.8^{+1.2}_{-1.2}$	$0.51^{+0.02}_{-0.02}$	with targets
2-8	$0.34^{+0.17}_{-0.17}$	$18.5^{+9.2}_{-9.2}$	$1.50^{+0.07}_{-0.07}$	$81.5^{+3.8}_{-3.8}$	$1.84^{+0.18}_{-0.18}$	

Note. — Col. (1): X-ray energy band in keV. Col. (2): the unresolved CXRB flux density (HM05) in units of 10^{-11} $erg\ cm^{-2}\ sec^{-1}\ deg^{-2}$. Col. (3): the percentage of the total CXRB flux density that is unresolved. Col. (4): the resolved CXRB flux density from the ChaMP+CDFs number counts in units of 10^{-11} $erg\ cm^{-2}\ sec^{-1}\ deg^{-2}$. The resolved CXRB in the 1-2 keV band is rescaled from that in the 0.5-2 keV band assuming $\Gamma_{ph}=1.4$. Col. (5): the percentage of the total CXRB flux density that is resolved. Col. (6): the total CXRB flux density in units of 10^{-11} $erg\ cm^{-2}\ sec^{-1}\ deg^{-2}$. This column is the sum of the column (2) and the column (4) for HM05 and this study. Col. (7): reference

Using the unresolved CXRB from the CDFs (Hickox & Markevitch 2006, ApJ, 645, 95, HM06) and the resolved CXRB from the ChaMP+CDFs, we estimated the total CXRB flux densities in 3 energy bands. **In each energy band, the resolved fraction of the CXRB is ~80%.** This fraction increases by ~1% when target sources are included.

This study agrees with HM06 within the uncertainties. Although this study presents somewhat lower resolved fractions than Morreti et al. (2003, ApJ, 588, 696) and Bauer et al. (2004, AJ, 128, 2048), this study generally consistent with earlier studies within their larger uncertainties.

VI. Conclusion

We present the ChaMP/ChaMP+CDFs number counts in multiple X-ray energy bands. The differential number counts are fitted by a broken power law and the breaks have differential fluxes in different energy bands. The origin of the break depending on energy band can be explained by the identical X-ray population(s) in each energy band. In all energy bands, the soft sources are responsible for the break in the differential number counts. A hard X-ray source becomes softer with increasing redshift, and so the hard source number counts do not include high redshift sources while the soft source number counts include both soft sources with full range of redshifts and intrinsically hard sources with high redshifts. Therefore, the soft sources show the break due to the cosmological evolutionary effects and mixture of X-ray populations. We estimated the resolved/total CXRB flux density in 3 energy bands. The resolved fraction of the CXRB is ~80% in each energy band.